

Controlled growth of Zn-polar ZnO epitaxial film by nitridation of sapphire substrate

Z. X. Mei and X. L. Du^{a)}

State Key Laboratory for Surface Physics, Institute of Physics, Chinese Academy of Sciences, Beijing 100080, China

Y. Wang

Beijing Laboratory of Electron Microscopy, Institute of Physics and Center for Condensed Matter Physics, Chinese Academy of Sciences, Beijing 100080, China

M. J. Ying, Z. Q. Zeng, H. Zheng, J. F. Jia, and Q. K. Xue

State Key Laboratory for Surface Physics, Institute of Physics, Chinese Academy of Sciences, Beijing 100080, China

Z. Zhang

Beijing University of Technology, Beijing 100022, China

(Received 22 November 2004; accepted 26 January 2005; published online 9 March 2005)

Surface nitridation is used to eliminate O-polar inversion domains and control the growth of single-domain Zn-polar ZnO film on sapphire (0001) substrate by rf-plasma-assisted molecular-beam epitaxy. It is found that the nitridation temperature is crucial for achieving quality AlN buffer layers and ZnO films with cation polarity, as demonstrated by *ex situ* transmission electron microscopy. Under optimal growth conditions, a 4×4 surface reconstruction was observed, which is confirmed to be a characteristic surface structure of the Zn-polar films, and can be used as a fingerprint to optimize the ZnO growth. © 2005 American Institute of Physics.

[DOI: 10.1063/1.1884266]

As a wide-band-gap oxide semiconductor, ZnO has enormous potential applications in short-wavelength optoelectronic devices. Many achievements have been made due to the fact that high-quality epitaxial layers are available by various methods.^{1–9} Polarity control is one of the most important issues for obtaining good crystalline quality, because the formation of inversion domains (IDs) in polar ZnO will severely deteriorate the material.^{10,11} In addition, recent studies demonstrate much higher *p*-type doping efficiency in Zn-polar films compared to O-polar ones.^{1,12} Although the origin of *p*-type conduction in Zn-polar ZnO films is not clear at present, it is very important to achieve controllable growth of Zn-polar ZnO films for light-emitting diode and laser diode applications.

Bulk ZnO is commercially available and Zn-polar ZnO homoepitaxy has been reported recently.^{13,14} Due to the high cost, rough surface morphology, and poor crystal quality of the ZnO substrate, however, α -Al₂O₃ (0001) is still the more favorable substrate currently used. The problem with sapphire is the formation of O-polar IDs. The pregrowth surface nitridation at low temperature was employed to obtain uniform O-polar ZnO growth on sapphire by molecular-beam epitaxy (MBE) in our previous work.¹⁵ A thin AlN layer formed on α -Al₂O₃ is found to effectively suppress Zn-polar IDs and promote O-polar film growth. In this work, we use this method to control the polarity of AlN and ZnO layers. Our finding is that uniform Zn-polar ZnO films could be controllably obtained by nitridation at a higher temperature (400–550 °C), as substantiated consistently by reflection high-energy electron diffraction (RHEED), convergent beam electron diffraction (CBED), and transmission electron microscopy (TEM) studies. This makes the films of this type

very promising for high concentration *p* doping.^{1,12}

Our ZnO samples were prepared on sapphire (0001) substrates using an rf-plasma-assisted MBE system (OmniVac). The base pressure in the growth chamber was $\sim 1 \times 10^{-10}$ Torr. Zn was supplied by evaporating 6N elemental Zn from a commercial Knudsen cell (CreaTech). Active oxygen and nitrogen radicals were produced by two rf-plasma systems (SVTA), respectively. The flow rate of oxygen/nitrogen gas was controlled by a mass flow controller (ROD-4, Aera).

After degreasing in trichloroethylene and acetone, the sapphire substrates were chemically etched for 30 min in a hot solution of H₂SO₄:H₃PO₄=3:1 at 110 °C and then rinsed with deionized water. Before growth, the substrates were thermally cleaned at 800 °C for 1 h, followed by nitridation at 400–550 °C for 1 h with an rf power of 480 W and a nitrogen flux of 3.0 sccm. Nitridation at either lower or higher temperatures was also investigated, but neither of them could lead to good-quality Zn-polar films. Then, conventional two-step growth of ZnO, i.e., a low-temperature (LT) buffer layer growth at 400 °C and a high-temperature growth at 650 °C, was performed. The in-plane epitaxial relationship, surface morphology evolution, and crystallinity were monitored *in situ* by RHEED. A Philips CM200 field emission gun transmission electron microscope, operating at 200 kV, was used for polarity determination and cross-sectional microstructure characterization.

We first describe the detailed growth processes of the ZnO epilayers based on *in situ* RHEED observation. Figures 1(a) and 1(b) show the RHEED patterns recorded before and after nitridation, respectively. A thin AlN layer forms with a 30° in-plane rotation of its lattice with respect to the substrate after nitridation, and the sharp streaky patterns become diffuse. The RHEED signal from sapphire still exists, which indicates a very small thickness (~ 2 nm) of the AlN layer.

^{a)} Author to whom correspondence should be addressed; electronic mail: xldu@aphy.iphy.ac.cn

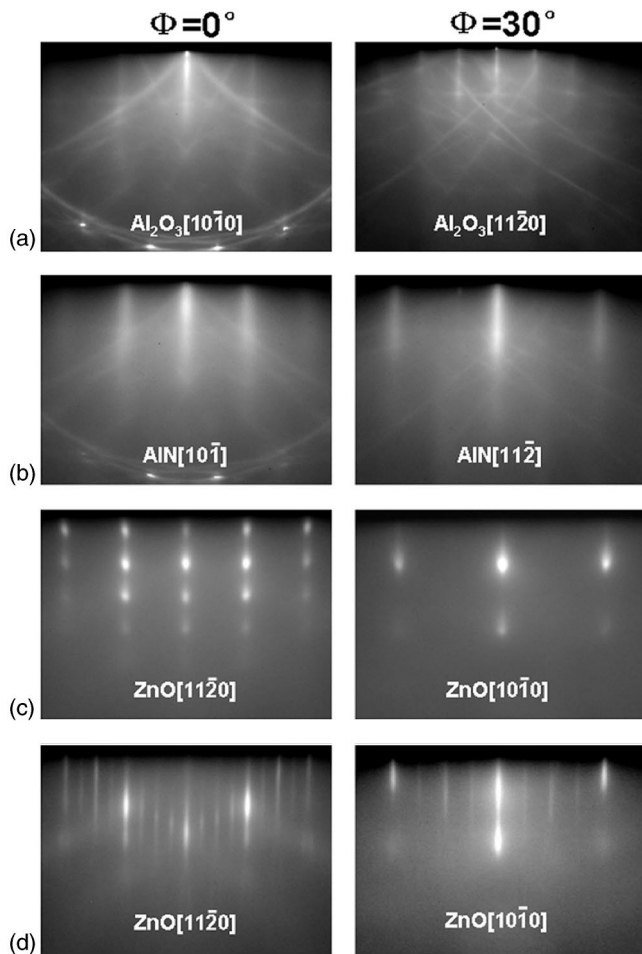


FIG. 1. RHEED patterns along $[10\bar{1}0]$ (the left panel) and $[11\bar{2}0]$ (the right panel) electron-beam azimuths obtained from (a) sapphire before nitridation, (b) sapphire after nitridation at 400–550 °C, (c) as-grown ZnO buffer layer at 400 °C, and (d) ZnO epilayer grown at 650 °C. A well-defined 4×4 reconstructed surface is observed in (d).

This thickness was further confirmed by the high-resolution TEM (HRTEM) observation. In addition, the diffuse RHEED patterns [Fig. 1(b)] suggest that the strain between AlN and sapphire is not relaxed. Similar to the case of O-polar ZnO, the AlN layer has a zincblende structure with stacking faults parallel to the AlN/Al₂O₃ interface.¹⁵ The diffuse patterns disappear once the LT ZnO buffer growth is initiated, and become spotty a few minutes later, with an in-plane epitaxial relationship of ZnO $[11\bar{2}0] // \text{AlN} [10\bar{1}]$ and ZnO $[10\bar{1}0] // \text{AlN} [11\bar{2}]$. During the LT buffer layer growth, the spotty patterns remain [Fig. 1(c)].

When the temperature ramps up to 650 °C, the RHEED patterns become streaky gradually. This situation could be dramatically promoted by interrupting the deposition and annealing at 750 °C. 10 min of annealing leads to very sharp streaky RHEED patterns, and more importantly, a well-defined 4×4 reconstruction is observed [Fig. 1(d)], which maintains for the entire deposition process. Previously, only two reconstructions (1×1 and 3×3) were observed. 3×3 reconstruction was reported in the growth of the O-polar ZnO films,^{16–18} where LT MgO and ZnO buffers were used. We found that, with pregrowth oxygen radical treatment and LT nitridation, the O-polar ZnO films could be also obtained with a characteristic 3×3 reconstructed surface.¹⁵ The surface reconstructs to optimize the surface energy, and differ-

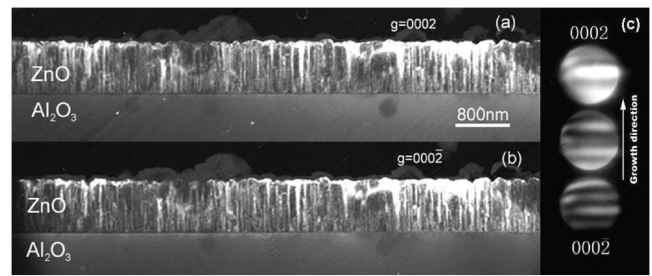


FIG. 2. Dark-field TEM images taken under (a) $g=0002$ and (b) $g=000\bar{2}$, and CBED pattern (c) of the ZnO thin film grown under optimal conditions.

ent surface stoichiometry and crystallographic orientation give rise to different stable surface structure, which can be a fingerprint of film polarity, such as the case of GaN(0001) and GaN(000 $\bar{1}$).^{19,20} Under this context, we speculate that the ZnO films may have a Zn polarity.

To confirm this, we carried out a TEM study of the sample prepared under the optimal conditions stated above. Figures 2(a) and 2(b) show the (0002) and (000 $\bar{2}$) dark-field images, respectively. No IDs are observed, and our sample is unipolar. The total density of threading dislocations in the sample is lower than $3 \times 10^9 \text{ cm}^{-2}$. A CBED pattern was then taken slightly away from the $[10\bar{1}0]$ zone axis toward $[11\bar{2}0]$ direction [Fig. 2(c)]. Since the (0002)_{Zn} face can reflect the electron beam much more strongly than the (000 $\bar{2}$)_O face, the central fringes at (0002) and (000 $\bar{2}$) disks should appear bright and dark, respectively.^{21,22} From the tokens in the CBED pattern [Fig. 2(c)], the ZnO film is determined to have [0001] polarity. The formation of an Al-polar AlN layer can thus be inferred. The dark-field images and CBED clearly show that the IDs of O polarity were effectively suppressed and a single-domain Zn-polar film was formed. Therefore, the 4×4 reconstruction is a characteristic structure of the Zn-polar ZnO film, and can be used as a fingerprint to identify the Zn polarity and conveniently establish the optimal growth conditions for high-quality Zn-polar ZnO films by *in situ* RHEED observation.

The HRTEM image along $[11\bar{2}0]_{\text{sapphire}}$ direction (see Fig. 3) clearly shows the interface microstructure between the nitridation layer and sapphire substrate. A continuous unrelaxed cubic AlN layer of $\sim 2 \text{ nm}$ thick was seen, which does not reduce the lattice mismatch between ZnO and sapphire (18.3%). It should be noted that the interface is smooth and sharp without any indication of interdiffusion or an amorphous structure. The zincblende AlN layer is confirmed to have an epitaxial relationship with $\alpha\text{-Al}_2\text{O}_3$ (0001) of

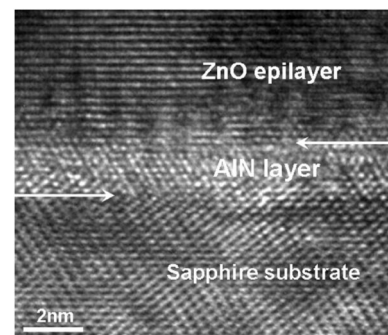


FIG. 3. HRTEM image taken along $[11\bar{2}0]_{\text{sapphire}}$ direction, which reveals the details of the interface microstructure of ZnO/AlN/sapphire.

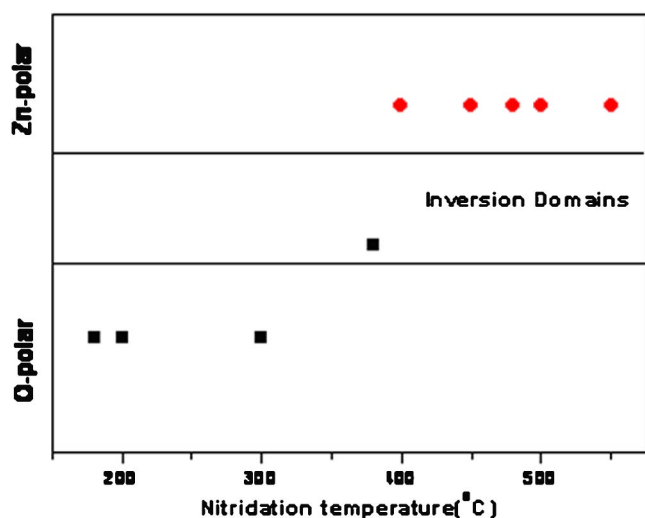


FIG. 4. Dependence of the ZnO film polarity as a function of the nitridation temperature, in which a wide nitridation temperature window (400 °C–550 °C) to achieve Zn-polar films is seen.

[111] AlN/[0001] Al₂O₃, and [11 $\bar{2}$] AlN/[11 $\bar{2}$ 0] Al₂O₃. More details can be found in our previous work.¹⁵ The correlation between substrate pretreatment and nitridation temperature and the microstructure of the nitridation layer, as well as its polarity, has been studied systemically and will be discussed elsewhere.

In our experiments, we found that nitridation temperature plays a key role in AlN polarity selection, interface microstructure, and ZnO polarity. Figure 4 shows the ZnO film polarity as a function of the nitridation temperature. It clearly reveals that under standard growth conditions, such as plasma power and growth rate, the nitridation temperature seems to be the single critical parameter to determine film polarity. If the nitridation was performed at an intermediate temperature (300–400 °C), IDs were observed in TEM dark-field images (not shown here). Nitridation at 300 °C and below leads to an O-polar ZnO film (see Fig. 4). On the other hand, if the temperature (for example, 750 °C) is too high, thermal decomposition of the AlN layer will become serious.²³ Nitridation temperature has a crucial influence on polarity, but must be controlled delicately. The surface structure of α -Al₂O₃ (0001) has been described in detail before.^{24–27} Since nitridation involves N diffusion into sapphire and substitution for O, and a continuous single-crystalline AlN layer forms on the substrate, it is reasonable to believe that the coordination of Al atoms at the interface determines the polarity. In the case of the nitridation at 400–550 °C, N atoms tend to directly bond to Al atoms at the interface, leading to a stacking sequence of Al \equiv N–Al \equiv O and an Al-polar AlN film. At a low nitridation temperature (<300 °C), the substitution of nitrogen for oxygen should take place, the AlN layer formed at the interface has a sequence of Al–N \equiv Al–O and is N polar. At intermediate temperatures (300–400 °C), Zn-polar and O-polar domains coexist and unipolar films cannot be obtained. These results indicate that the temperature facilitated kinetic process could

be manipulated to control the interface bonding configuration and, thus, the polarity.

In summary, the role of nitridation temperature in the polarity selection of ZnO films was systematically examined by RHEED, CBED, and TEM. A 4 \times 4 surface reconstruction was observed, which we show can be used as a fingerprint for the growth of uniform Zn-polarity ZnO films on sapphire.

This work is supported by the National Science Foundation (Grant Nos. 60476044, 60376004, 60021403, 10174089) and the Ministry of Science and Technology (Grant No. 2002CB613502) of China.

¹X.-L. Guo, J.-H. Choi, H. Tabata, and T. Kawai, *Jpn. J. Appl. Phys.*, Part 2 **40**, L177 (2001).

²Y. R. Ryu, T. S. Lee, J. H. Leem, and H. W. White, *Appl. Phys. Lett.* **83**, 4032 (2003).

³H. Ohta, M. Orita, M. Hirano, and H. Hosono, *J. Appl. Phys.* **89**, 5720 (2001).

⁴H. Ohta, H. Mizoguchi, M. Hirano, S. Narushima, T. Kamiya, and H. Hosono, *Appl. Phys. Lett.* **82**, 823 (2003).

⁵H. Ohta, M. Hirano, K. Nakahara, H. Maruta, T. Tanabe, M. Kamiya, T. Kamiya, and H. Hosono, *Appl. Phys. Lett.* **82**, 1029 (2003).

⁶Y. I. Alivov, J. E. Van Nostrand, D. C. Look, M. V. Chukichev, and B. M. Ataev, *Appl. Phys. Lett.* **83**, 2943 (2003).

⁷Y. I. Alivov, D. C. Look, B. M. Ataev, M. V. Chukichev, V. V. Mamedov, V. I. Zinenko, Y. A. Agafonov, and A. N. Pustovit, *Solid-State Electron.* **48**, 2343 (2004).

⁸Y. I. Alivov, E. V. Kalinina, A. E. Cherenkov, D. C. Look, B. M. Ataev, A. K. Omaev, M. V. Chukichev, and D. M. Bagnall, *Appl. Phys. Lett.* **83**, 4719 (2003).

⁹K. Ip, Y. W. Heo, D. P. Norton, S. J. Pearton, J. R. LaRoche, and F. Ren, *Appl. Phys. Lett.* **85**, 1169 (2004).

¹⁰I. Ohkubo, A. Ohtomo, T. Ohnishi, Y. Mastumoto, H. Koinuma, and M. Kawasaki, *Surf. Sci.* **443**, L1043 (1999).

¹¹K. Nakahara, H. Takasu, P. Fons, K. Iwata, A. Yamada, K. Matsuura, R. Hunger, and S. Niki, *J. Cryst. Growth* **227**, 923 (2001).

¹²D. C. Look, D. C. Reynolds, C. W. Litton, R. J. Jones, D. B. Eason, and G. Cantwell, *Appl. Phys. Lett.* **81**, 1830 (2002).

¹³H. Kato, M. Sano, K. Miyamoto, and T. Yao, *Jpn. J. Appl. Phys.*, Part 2 **42**, L1002 (2003).

¹⁴H. Matsui, H. Saeki, T. Kawai, A. Sasaki, M. Yoshimoto, M. Tsubaki, and H. Tabata, *J. Vac. Sci. Technol. B* **22**, 2454 (2004).

¹⁵Z. X. Mei, Y. Wang, X. L. Du, M. J. Ying, Z. Q. Zeng, H. Zheng, J. F. Jia, Q. K. Xue, and Z. Zhang, *J. Appl. Phys.* **96**, 7108 (2004).

¹⁶Y. F. Chen, H.-J. Ko, S.-K. Hong, and T. Yao, *Appl. Phys. Lett.* **76**, 559 (2000).

¹⁷Y. F. Chen, H.-J. Ko, S.-K. Hong, T. Yao, and Y. Segawa, *J. Cryst. Growth* **214**, 87 (2000).

¹⁸K. Iwata, P. Fons, S. Niki, A. Yamada, K. Matsuura, K. Nakahara, and H. Takasu, *Phys. Status Solidi A* **180**, 287 (2000).

¹⁹Q. K. Xue, Q. Z. Xue, R. Z. Bakhtizin, Y. Hasegawa, I. S. T. Tsong, T. Sakurai, and T. Ohno, *Phys. Rev. Lett.* **82**, 3074 (1999).

²⁰A. R. Smith, R. M. Feenstra, D. W. Greve, J. Neugebauer, and J. E. Northrup, *Phys. Rev. Lett.* **79**, 3934 (1997).

²¹P. Han, Z. Wang, X. F. Duan, and Z. Zhang, *Appl. Phys. Lett.* **78**, 3974 (2001).

²²Y. Wang, Q. Y. Xu, X. L. Du, Z. X. Mei, Z. Q. Zeng, Q. K. Xue, and Z. Zhang, *Phys. Lett. A* **320**, 322 (2004).

²³Z. Y. Fan and N. Newman, *Mater. Sci. Eng.*, B **87**, 244 (2001).

²⁴E. A. Soares, M. A. Van Hove, C. F. Walters, and K. F. McCarty, *Phys. Rev. B* **65**, 195405 (2002).

²⁵T. J. Godin and J. P. LaFemina, *Phys. Rev. B* **49**, 7691 (1994).

²⁶C. F. Walters, K. F. McCarty, E. A. Soares, and M. A. Van Hove, *Surf. Sci.* **464**, L732 (2000).

²⁷J. Guo, D. E. Ellis, and D. J. Lam, *Phys. Rev. B* **45**, 13647 (1992).